

Bacteriorhodopsin Intermediate Spectra Determined over a Wide pH Range

Csilla Gergely,* László Zimányi, and György Váró

*Institute of Biophysics, Biological Research Centre of the Hungarian Academy of Sciences,
H-6701 Szeged, Hungary*

Received: April 24, 1997

The pH dependence of the absorption spectra of bacteriorhodopsin and its photocycle intermediates was studied in the pH range 4.5–9. The spectra of the intermediates were determined from difference spectra taken during the photocycle with an optical multichannel analyzer. The data analysis was based on various criteria concerning the shape of the spectra, but no assumption was made about the kinetic model that describes the photocycle. The strategy for calculation of the spectra was one described earlier, as well as a newly introduced algorithm based on the Monte Carlo method. The search methods used gave very similar results. Like the absorption spectrum of bacteriorhodopsin in the above-mentioned pH range, the spectra of all the intermediates were found to be almost unchanged. The spectrum of intermediate M displayed a 2 nm, and that of intermediate L a 1 nm, red shift with rising pH, but this latter shift was within the overall error of the measurements. The similarity of all the intermediate spectra calculated with different procedures at all pH values points to the reliability of the method and the validity of the spectra. Averaging of the calculated spectra over the whole pH range furnished a well-determined set of intermediate spectra, suitable for further kinetic and spectroscopic studies of the photocycle.

Introduction

Bacteriorhodopsin (BR), the only protein in the purple membrane of *Halobacterium salinarum*, functions as a light-driven proton pump.^{1–3} Its structure is known with 0.35 nm resolution.^{4,5} Upon absorbing light the retinal chromophore of BR passes through an excited state to a higher-energy state, and a series of thermal reactions drive the protein through several spectrally distinct intermediates (denoted K, L, M, N, and O) back to the initial form, BR. Most of the intermediates have been decomposed kinetically to several spectroscopically indistinguishable substates. Recent reviews describe the details of the photocycle and the related proton pumping mechanism.^{3,6,7}

The pH dependence of the BR spectrum has been investigated intensively. When the pH of the purple membrane suspension is mentioned, it must be borne in mind that it is usually measured in the bulk, but, depending on the ionic strength of the solution, the pH at the membrane surface will be lower due to the negative surface charge. When the ion concentration of the suspension is lowered, this difference increases and can reach several pH units.⁸ In the pH interval 4–9 at moderate ionic strength (several hundred mM), where the surface pH is presumed to be approximately equal to that measured in the bulk, the spectra of the ground-state BR are considered practically unchanged.^{9,10} At pH below 4, BR passes through a series of transformations, depending on the nature and concentration of the ions in the suspension.^{11–13} One very pronounced change is the transition from purple to blue membrane with a pK_a 2.5 when no chloride is present.¹³ At pH above 9, the deprotonation of some amino acids produces a smaller spectral change,^{12,14,15} and at even higher pH the Schiff base can deprotonate without illumination. Recent findings show that there is a spectral change with pK_a around 9.7, a secondary transition of the blue to purple membrane, which can be observed only at long wavelengths, around 700 nm. The explanation of the two pK_a 's is based on

the complex titration of residue D85 together with another proton acceptor group in the extracellular half-channel of BR.¹⁶

The first attempts to determine the spectra of the photocycle intermediates were performed by trapping the BR sample in different intermediate states at low temperature.^{17,18} With the introduction of the optical multichannel analyzer, the possibility arose for the detection of the whole spectral change at a given time after excitation and for calculation of the spectra of the intermediates.^{19–21}

Investigations of the effect of pH upon the BR photocycle (for a review, see ref 7) assume that the spectra of the intermediates are pH-independent,^{21,22} but the validity of this hypothesis has never been proven. In the present work, this question was investigated in the pH range from 4.5 to 9, where the spectrum of BR can be considered to be unchanged. The spectra of the intermediates were calculated without any assumption concerning the kinetic model of the photocycle, but several hypotheses regarding the shape of the spectra were used: non-negative absorption, smooth spectra, only one main peak, and shapes resembling the skewed spectra of the rhodopsin-type pigments.^{23–25} The spectra were unchanged or only slightly affected by the pH change. The spectrum of intermediate M shifted toward the red by about 2 nm and that of L intermediate by about 1 nm in the same direction as the pH was raised, but the latter shift was within the overall error of the analysis.

Materials and Methods

Purple membranes were isolated from *H. salinarum* strain Sg by the standard procedure described previously.²⁶ The isolated purple membranes were embedded in polyacrylamide gel, by means of a method reported elsewhere,¹¹ having a BR concentration of about 15 μ M. The gel was soaked overnight in 100 mM NaCl, 25 mM Bis–Tris propane, and 25 mM phosphate buffers at the desired pH. It was light-adapted prior to the measurement and thermostated at 20 °C during data collection. Absorption spectra of the light-adapted BR contain-

* Corresponding author. E-mail: Gergelycs@everx.szbk.u-szeged.hu.
Fax: 36-62-433133.

† Abstract published in *Advance ACS Abstracts*, October 15, 1997.

ing gels were measured in a Shimadzu spectrophotometer and revealed no pH dependence in the studied pH range (data not shown).

Time-resolved spectroscopy with a gated optical multichannel analyzer (OMA), as described elsewhere,²⁰ provided difference spectra at various time points during the photocycle. The exciting laser flash was monitored by a home-built power meter, and all the data were normalized to the same laser intensity.

Data Analysis

Singular Value Decomposition. In addition to the difference spectra, noise spectra were measured for each instrumental setting without gating the OMA detector. Increasing delay times allowed longer gate pulses and hence less noisy spectra. The noise also depended on the varying light intensity over the wavelength range due to spectral variations of the measuring light source, absorption of the sample, and spectral sensitivity of the detector. Hence the data matrix of the measured difference spectra was nonuniform with respect to noise along both the time and the wavelength dimensions. Estimation of the variations of the noise based on the measured noise spectra was used to correct the data matrix along both dimensions to attain a modified data matrix with uniform noise. The corrected difference spectra were then subjected to singular value decomposition (SVD).^{27,28}

$$\mathbf{D} = \mathbf{U} \cdot \mathbf{S} \cdot \mathbf{V}^T \quad (1)$$

where \mathbf{D} ($n \times m$) is the data matrix with m difference spectra arranged in columns, \mathbf{U} ($n \times m$) contains the orthonormal abstract basis spectra, \mathbf{S} ($m \times m$) diagonal matrix consists of the singular values, \mathbf{V} ($m \times m$) contains the orthonormal abstract kinetic vectors, n is the number of wavelength values, and m is the number of time points.

SVD analysis gave the lower limit, r , of the number of spectrally distinct intermediates present in the photocycle. This was determined using two criteria:²⁷ (i) the sum of the squared singular values beyond the first r ones should be less than the estimated total squared noise content of the data matrix calculated from the measured noise spectra, and (ii) the autocorrelation of the first r columns of the \mathbf{U} and \mathbf{V} matrices should be higher than a threshold value of 0.6. The autocorrelation for the spectral vectors was calculated using a 9 nm shift since the spectra contain a noise pattern with a high short distance autocorrelation. This is due to the fixed pattern noise of the detector and the "spillover" of the signal between neighboring diodes of the array.

Once r had been determined, the data matrix was reconstructed using only the first r singular values and columns of \mathbf{U} and \mathbf{V} . Next the correction based on the noise was reverted to yield the noise filtered spectral data matrix.

Monte Carlo Search for the Pure Intermediate Spectra. The spectral data matrix is the product of the difference spectra and the time-dependent concentrations (kinetics) of the pure intermediates, both unknown:

$$\mathbf{D} = \Delta\epsilon \cdot \mathbf{c}^T \quad (2)$$

Multiplying with the pseudo-inverse of the transpose of the concentration matrix \mathbf{c} yields the difference spectra of the intermediates:

$$\mathbf{D} \cdot \mathbf{c} \cdot (\mathbf{c}^T \cdot \mathbf{c})^{-1} = \Delta\epsilon \quad (3)$$

In the Monte Carlo algorithm elements of the concentration matrix \mathbf{c} were generated randomly using weak (model-

independent) criteria. These were (1) Each concentration value must be between zero and one. (2) The concentration of the K intermediate must decrease monotonously due to the fact that the formation of K is much faster than the time resolution of our measurement. (3) Once the concentration of any other intermediate has started to decrease it cannot increase again. (4) Limits were introduced for the maximal change of the concentration of each intermediate between consecutive time points (too abrupt changes were not allowed), as required by first-order processes. (5) The sum of the concentrations at each time point, with the concentration of the fraction of recovered BR initial state included, must be close to 1. Another parameter, the fraction of photoexcited molecules (photocycling ratio), was also randomly varied in the search procedure.

For each random concentration matrix the respective intermediate difference spectra were calculated using eq 3 and the absolute spectrum of BR, normalized by the photocycling ratio, added. The assumption, which was tested on simulated data (not shown), was that once the generated \mathbf{c} is close enough to the (unknown) actual \mathbf{c} , the calculated $\Delta\epsilon$ is a good approximation of the pure intermediate spectra. The resulting prospective pure intermediate spectra were subjected to increasingly stringent criteria regarding their shape, maximum, etc.,²⁵ as follows: (a) Absolute spectra must be nonnegative (a threshold of small negative extinctions was introduced because of the noise). (b) The spectra must have a single, major absorption band without additional red-shifted minor bands or shoulders. The position of the maxima were limited within intervals based on previous knowledge about the BR intermediate spectra. (c) The full width at half-maximum of the intermediate absolute spectra as well as their maximal amplitudes were also limited within reasonable intervals. (d) Except for the M intermediate, all other intermediates' extinction was limited within intervals close to the extinction of BR in the spectral region of 370–430 nm.

The difference spectra were divided into two subsets. The first subset included the spectra up to the point where intermediate M reached its maximal concentration, containing only intermediates K, L, and M. The second subset in general contained diminishing contributions from K and L, as well as contributions from the M, N, and O intermediates. The first subset was subjected to the Monte Carlo search method to determine the photocycling ratio and the spectra of K, L, and M intermediates. These spectra were considered as known parameters during the analysis of the second subset when the N and O spectra were searched for. As a test a grid search over the "space" of the concentration values, already described elsewhere,²⁵ was also performed, and the results were compared with the new Monte Carlo search method. The grid search procedure failed in calculations of the spectra of the intermediates from the second subset of difference spectra, when the photocycle contained not only intermediates K, L, and M but also O and N. In this case, the earlier-described trial and error method was used as a test.²⁴ The Monte Carlo method was applicable to this subset of data as well and yielded acceptable N and O spectra.

Results

The photocycle of BR was measured in the time interval 200 ns to 600 ms by taking 25–33 difference spectra at logarithmically equidistant time points. Such sets of spectra were collected at 10 values in the pH interval 4.5–9. A representative set taken at pH 7 is presented in Figure 1. The decay of the red-shifted K intermediate is observed in the first part of the photocycle (Figure 1A), leading to an increase at around 500

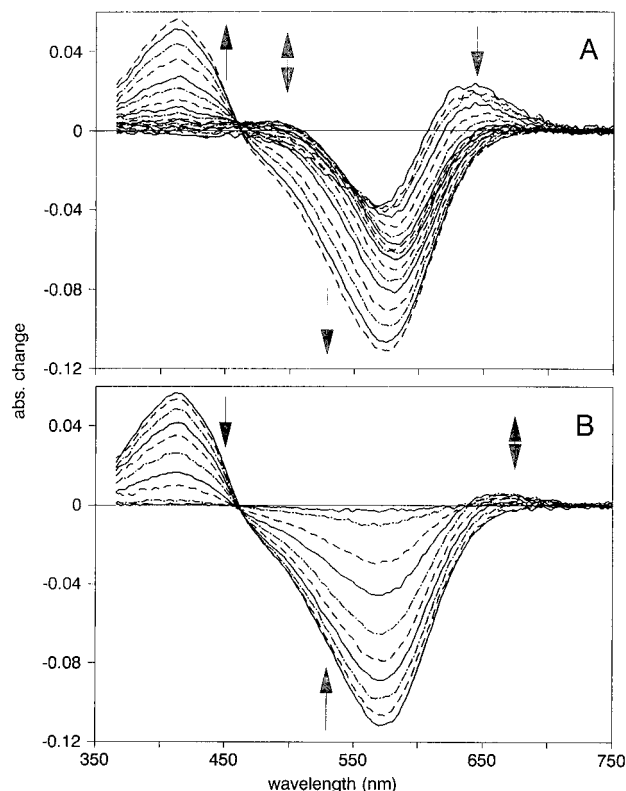


Figure 1. Difference spectra measured in 100 mM NaCl, 25 mM phosphate, and 25 mM Bis-Tris propane buffer at pH 7 and 20 °C: (A) difference spectra measured up to the time when intermediate M reaches its maximum concentration at about 400 μ s; (B) difference spectra measured in the second half of the photocycle (600 μ s–40 ms). The arrows show the direction of change of the spectra with increasing time.

nm, due to the appearance of intermediate L, and a later decrease in this region gives rise to increase at around 400 nm, corresponding to the transition from L to M intermediate. In the second part of the photocycle (Figure 1B), during the decay of the M intermediate there is a change in the ratio between the 400 and 570 nm peaks, because of intermediate N, and a rise and decrease at around 650 nm, corresponding to the O intermediate. At different pH values, the overall sequence of the photocycle is almost the same, with moderate changes in the rise and decay times, resulting in differences in the shapes of the difference spectra.

Each set of difference spectra was subjected to SVD analysis. It was found that at all 10 pH values four representative spectra (Figure 2A) and the corresponding amplitudes (Figure 2B) passed both the noise and the autocorrelation tests and described the whole set of spectra adequately. As an example, the pair product of the autocorrelations of the first five SVD components of the data measured at pH 7 had the values 0.97, 0.92, 0.77, 0.72, and 0.27. Noise-filtered difference spectra could be reconstructed from these four SVD components.

For computational reasons, only five difference spectra were chosen from the whole set (Figure 3) at times where one of the intermediates dominates. (At some, but not all, pH values the Monte Carlo method was tested including all difference spectra of the first subset of the data matrix and yielded similar K, L, and M spectra to those obtained from the truncated data matrix.) At every pH value the subset consisting of the first three spectra, up to the time when M reaches its maximum, was used to calculate the spectra of K, L, and M. The grid search and the Monte Carlo method gave similar results. The value of the photocycling ratio turned out to be around 0.26 in all measure-

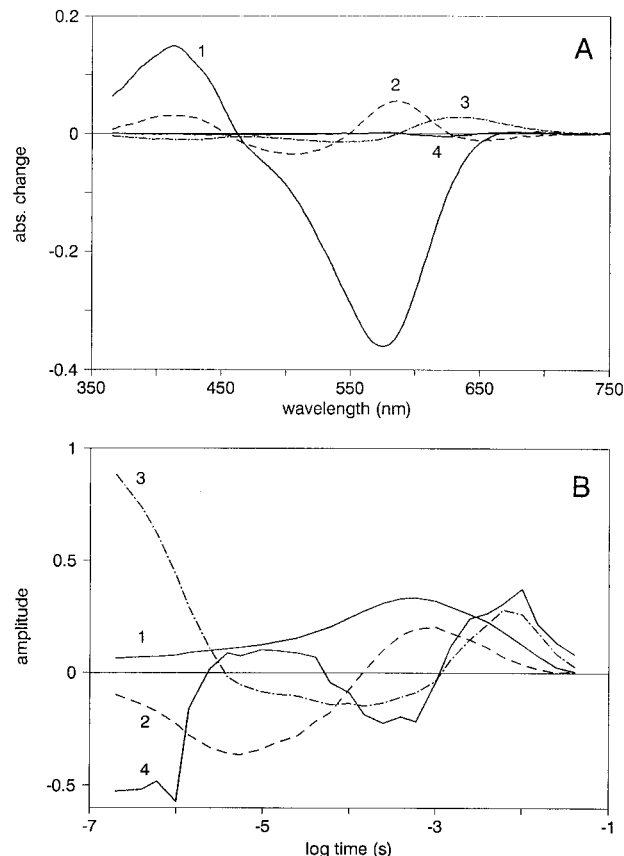


Figure 2. Characteristic spectral (A) and kinetic components (B) of the SVD analysis of the difference spectra measured at pH 7 and shown in Figure 1.

ments, demonstrating indirectly that the quantum yield of the BR photocycle is pH-independent in the studied range.^{29,30} Spectral searches for intermediates N and O were performed on the last two spectra of the set of five (Figure 3), using the spectra of the earlier intermediates as known. Since intermediate N does not accumulate at low pH,^{21,31} its spectrum could not be determined below pH 5.5. At high pH intermediate O vanishes; it was impossible to determine its spectrum above pH 8. The Monte Carlo and the grid search methods yielded multiple solution sets of acceptable intermediate spectra depending on the processing time for the former and the fineness of the grid for the latter, as well as the selected tolerance values of the criteria for the shape of the spectra. The resulting spectral sets were evaluated on the basis of two parameters: (1) the least-squares difference between the entire spectral data matrix and the fit of the matrix using the calculated intermediate spectra with the constraint of nonnegative concentrations and (2) the deviation of the so-obtained concentration sums from the expected value of 1. The best 10 solutions for each pH were retained and showed little variance, permitting their averaging to yield a single intermediate spectral set at each pH.

In the studied pH range, the so-obtained spectra displayed a random variation of about $\pm 5\%$ in their amplitude (not shown). The position of the maximum also exhibited a random variation of about 4 nm for almost all the intermediates. Figure 4 shows the position of the maximum for the intermediates calculated with the Monte Carlo method. The grid search and the trial and error calculation gave similar results (not shown). The spectrum of intermediate M was determined with the least error (less than 0.3 nm), since its blue-shifted main absorption band does not overlap with that of BR or any other intermediate and it accumulates in a large amount. Its maximum shifted from

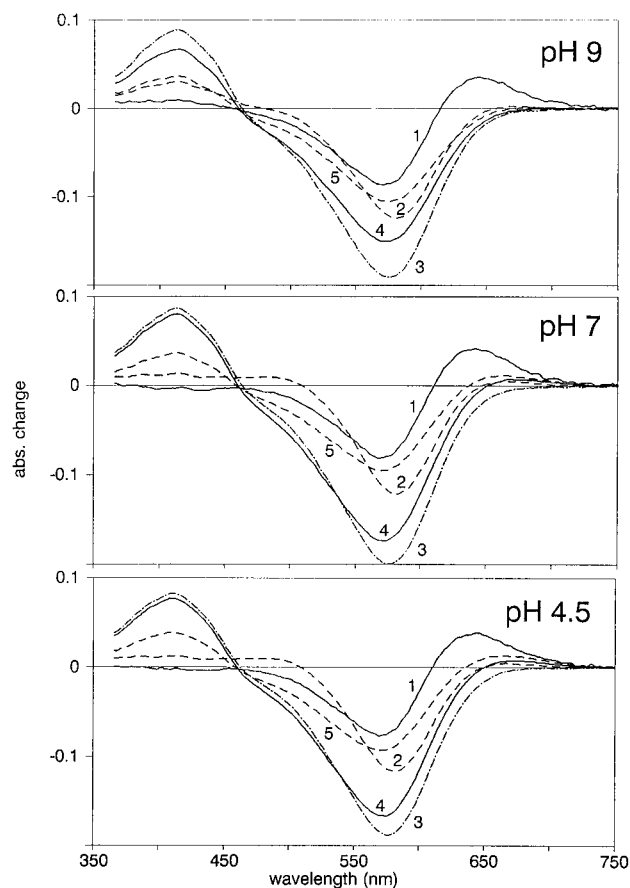


Figure 3. Difference spectra used in the search for the spectra of the intermediates, at three different pH values. The delay times for the spectra are: (1) 400 ns, (2) 5.5 μ s, (3) 150 μ s, (4) 2.5 ms, (5) 10 ms. Measuring conditions were as in Figure 1.

408 nm at pH 5 to 410.5 nm at pH 9. Greater uncertainties in the calculation were met for intermediates K, L, and N due to their strong overlap with the BR spectrum. The most uncertain was the spectrum of the O intermediate, as it accumulates in only a very small amount and at the end of the photocycle, when the reappearance of the initial form of BR also has to be taken into account. Although the position of the maximum for intermediate L was determined with an error of about 3 nm, the fit of the maximum reveals a slight pH dependence (Figure 4). The reality of this shift is not certain, as it is within the error of the measurement. As the positions of the maxima for intermediates K, N, and O involved an uncertainty larger than 4 nm and did not show any tendency with pH, it can be stated that, if they do depend on pH, their variation is less than 4 nm.

In the last step, the average of the obtained spectra at different pH values for every intermediate was calculated for both the grid search (for K, L, M) combined with trial and error method (for N, O) and Monte Carlo methods. Finally these two sets of intermediate spectra were compared. The difference between the spectra of the first three intermediates determined by the two methods was less than 2%. The O spectrum calculated by the first method was noisy, due to its low concentration during the photocycle. To improve it, this spectrum was filtered by fitting it with five Gaussian curves. For intermediate N, the Monte Carlo method gave a spectrum about 5% smaller than that calculated by trial and error, but with its maximum at exactly the same position. For intermediate O this difference was larger, at around 15%. As all the other spectra were within the limit of error and the spectrum of O was the most uncertain, we averaged all the spectra calculated by the two methods for the given intermediate (Figure 5). The calculated spectra were

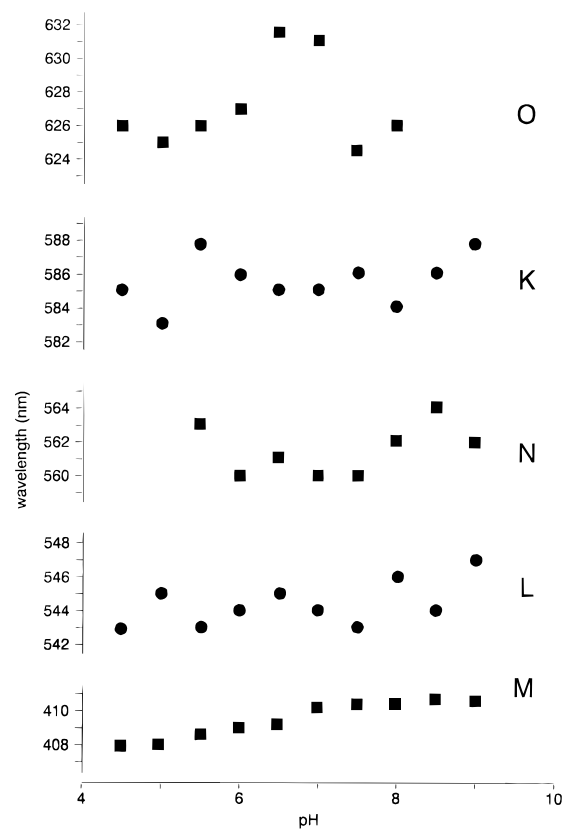


Figure 4. Wavelength of the maxima obtained for the spectra of the intermediates determined at different pH values.

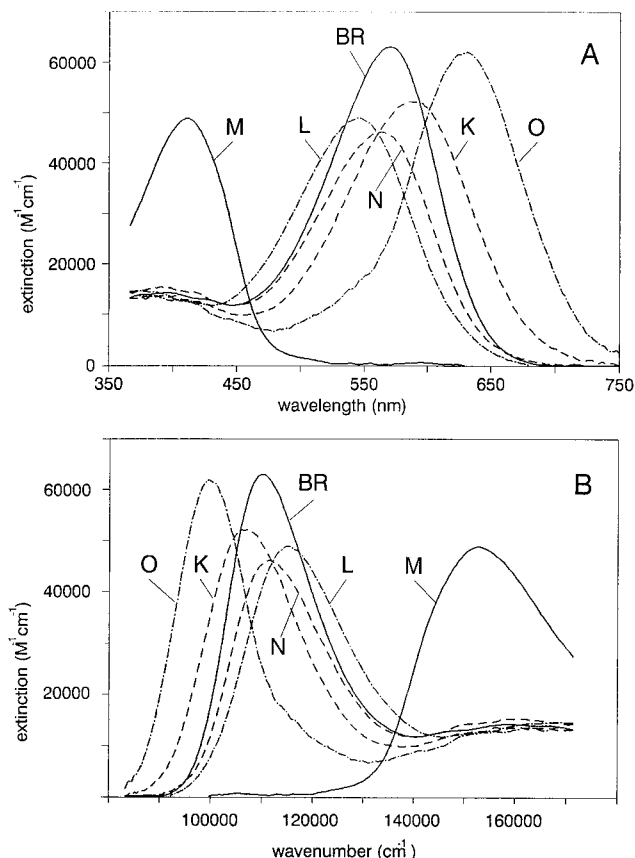


Figure 5. Spectra of the intermediates averaged over 10 pH values, presented as functions of wavelength (A) and wavenumber (B).

fitted back to all the measured difference spectra, and this resulted in a very good fit and acceptable kinetics for the intermediates.

Figure 5 presents the spectra as functions of wavelength (A), which is the usual representation, and wavenumber (B), as used in spectral and molecular dynamics calculations.

Discussion

SVD analysis of the data sets at all pH values gave four significant spectra and related kinetics, suggesting that at least four spectrally different intermediates are present in the photocycle. The fact that except for the low and high pH extremes there are five intermediates in the photocycle can be reconciled with the result that four SVD components were sufficient to represent the data. At the noise level of our measurement the fifth SVD component became nonsignificant because of the low (but nonnegligible) concentration of intermediate O and the relative spectral similarity of the O and K, as well as the L and N, spectra. In the spectral search the input spectra were the (SVD-reconstituted) measured difference spectra (see eq 3); therefore, the number of SVD components considered did not play a role in the following analysis. On the basis of criterion i of the SVD treatment (see above), the input data were reconstructed within noise, as was also confirmed by visual comparison of the original and SVD-reconstructed spectra. Less than five intermediates, except for the extreme pH values, would clearly violate rule 3 in the Data Analysis section above, requiring a rise in the concentration of at least one of the intermediates after its (partial) decay. The fact that four SVD spectra can describe the contribution of five real spectra is by no means contradictory, since the SVD spectra are orthonormal, whereas the real ones are generally nonorthogonal vectors in the space of the basis set consisting of the abstract SVD spectra.

More than five intermediates may contribute to the photocycle (substates of the major intermediates); however, our analysis was not sensitive enough to enable a clear distinction between them.

The measurements at 10 different pH values were handled separately but analyzed in exactly the same way. Little variation in the photocycle kinetics in the measured pH range afforded a possibility to use the same time points for the spectral search at each pH value (Figure 3). The changes observed between the spectra at the same time points at different pH values are due to the different concentrations of the intermediates, and not to spectral shifts, as the spectra of the intermediates proved to be almost pH independent. It is interesting that the two search methods for intermediates K, L, and M gave very similar spectra to those found earlier for wild type BR by a trial and error method.²⁴ Spectra of K, L, and M have been obtained recently for the D96N mutant BR by the grid search method²⁵ later combined with additional kinetic and stoichiometric criteria,³² and show good overall agreement with the ones reported here.

The only consistent monotonous pH-dependent change is observed for the spectrum of intermediate M. There are two possible explanations for the change: (1) M substates, in successive pathways ($M_1 \rightleftharpoons M_2$)^{24,33} or parallel pathways (M_f and M_s),^{34–36} have slightly different spectra, and their relative contributions to the total M is pH dependent for kinetic reasons, or (2) the spectrum of M itself shifts with pH. To decide between these two possibilities, the results of measurements at pH 9 were examined. It is known,^{33,35} that at high pH there is a fast rise in M, its quantity reaches a maximum plateau, and the decay is slow. In the case of the sequential photocycle model, it has been shown that at high pH mostly M_1 is present during the rise, whereas mostly M_2 can be observed during the decay.³³ In the case of parallel photocycles, the two M's appear together, but M_f decays faster.³⁵ In both cases, the ratios of the two M's in the rising and falling phases should be different

TABLE 1: Values of Wavelength Maximum, Extinction Coefficient, and Half-Width for the Spectra of the Intermediates

intermediates	λ_{\max} (nm)	ϵ_{\max} ($M^{-1} \text{ cm}^{-1}$)	Δk (cm^{-1})
BR	570	63.0×10^3	20.4×10^5
K	586	52.1×10^3	22.3×10^5
L	544	48.9×10^3	24.3×10^5
M	409	48.8×10^3	33.3×10^5
N	562	46.1×10^3	22.6×10^5
O	629	61.9×10^3	14.6×10^5

and a shift in the maximum at around 400 nm with time should be observed if the first assumption is valid. Since in the 400 nm region only the M intermediate contributes to the difference spectra, the position of the maximum of the difference spectra can be considered identical to that of the absolute M spectrum. A careful analysis of the difference spectra (both original and SVD reconstituted) demonstrated that, within 1 nm, there was no shift in the maximum (not shown). This negative result makes explanation 2 more likely.

After the L intermediate, the Schiff base becomes deprotonated, which results in more localized π -electrons of the retinal,^{37,38} reflected in the broadening and a shift toward higher wavenumbers of the M spectrum relative to BR (Figure 5B). This would mean that any change in the environment of the retinal will cause less variation in its spectrum.³⁷ Nevertheless elevation of the external pH in the range from 4.5 to 9 results in monotonous shift in the M spectrum (Figure 4). This shift may be caused by the titration of some surface amino acids or by an electrostatic effect upon the membrane surface. As the pH is raised, the membrane surface double layer is altered, giving rise to a continuous change in the electric field across the membrane. No explanation was found as to why this electrostatic effect influences the spectrum of the M state and not the spectra of the other, supposedly more sensitive intermediates with protonated Schiff bases. It is possible that they also undergo a shift, but that this is concealed by the uncertainty in the analysis, although no shift was observed for the BR initial state either. Another explanation to be tested in future work could be a transient protonation change in the membrane during the lifetime of the M intermediate.

Although the computation error of the M spectrum is less than 0.3 nm, the overall error of the whole analysis is about 4 nm, as it was described earlier, which allows to use even for the M intermediate an average spectrum.

In the spectrum of intermediate O, a weak shoulder appears at around 530 nm (Figure 5). This may be due to the strong temporal overlap of intermediates N and O, with some N spectrum accompanying the spectrum of O. Spectrally, this is only a 1–2% contribution, which corresponds to a concentration change of a fraction of a percent between the intermediates N and O. Our analysis is not sensitive enough to rule out such a small amount of N.

The characteristic parameters from the spectra of the intermediates are presented in Table 1. The maximum extinction coefficient decreases until N, but the O intermediate has almost the same value as BR. In several previous publications, the calculated spectrum of intermediate O was higher than that of BR.^{19–21} We assume that the O spectrum from Figure 5 is most probably the correct one, as it is an average of eight spectra from the pH range 4.5–8, calculated by two different methods.

The significance of the present results is in the (model-independent) determination of the intermediate spectra of bacteriorhodopsin over a wide pH range. The extinction values obtained can be used in future work to fit high temporal resolution single (or multiple) wavelength absorption kinetic

traces. These data combined with photoelectric or vibrational spectroscopic measurements may provide the necessary information to arrive at a unique reaction scheme of the BR photocycle and, potentially, at a proton pump mechanism. The accuracy of the K, L, and M spectra obtained here seems already sufficient, whereas that of the N and O spectra may be improved by analyzing mutants where these intermediates accumulate in higher amounts than in wild type.

Acknowledgment. The authors are grateful to J. K. Lanyi and A. Dér for valuable discussions. This work was supported by grants from the National Science Research Fund of Hungary (OTKA T020470 and T022066). The spectra of the intermediates are available on request from the authors in ASCII file format.

References and Notes

- (1) Krebs, M. P.; Gobind Khorana, H. J. *Bacteriol.* **1993**, *175*, 1555–1560.
- (2) Lanyi, J. K. *Biochim. Biophys. Acta Bioenergetics* **1993**, *1183*, 241–261.
- (3) Ebrey, T.; Jackson, M., Eds.; *Thermodynamics of membranes, receptors and channels*; CRC Press: New York, 1993; p 353–87.
- (4) Ceska, T. A.; Henderson, R.; Baldwin, J. M.; Zemlin, F.; Beckmann, E.; Downing, K. *Acta Physiol. Scand.* **1992**, *146* (Suppl. 607), 31–40.
- (5) Grigorieff, N.; Ceska, T. A.; Downing, K. H.; Baldwin, J. M.; Henderson, R. *J. Mol. Biol.* **1996**, *259*, 393–421.
- (6) Lanyi, J. K. *J. Bioenerg. Biomembr.* **1992**, *24*, 169–179.
- (7) Lanyi, J. K.; Váró, G. *Isr. J. Chem.* **1995**, *35*, 365–385.
- (8) Szundi, I.; Stoekenius, W. *Biophys. J.* **1989**, *56*, 369–383.
- (9) Maeda, A.; Takeuchi, Y.; Yoshizawa, T. *Biochemistry* **1982**, *21*, 4479–4483.
- (10) Kimura, Y.; Ikegami, A.; Stoekenius, W. *Photochem. Photobiol.* **1984**, *40*, 641–646.
- (11) Mowery, P. C.; Lozier, R. H.; Chae, Q.; Tseng, Y. W.; Taylor, M.; Stoekenius, W. *Biochemistry* **1979**, *18*, 4100–4107.
- (12) Muccio, D. D.; Cassim, J. Y. *J. Mol. Biol.* **1979**, *135*, 595–609.
- (13) Váró, G.; Lanyi, J. K. *Biophys. J.* **1989**, *56*, 1143–1151.
- (14) Bashford, D.; Gerwert, K. *J. Mol. Biol.* **1992**, *224*, 473–486.
- (15) Száraz, S.; Oesterhelt, D.; Ormos, P. *Biophys. J.* **1994**, *67*, 1706–1712.
- (16) Balashov, S. P.; Imasheva, E. S.; Govindjee, R.; Ebrey, T. G. *Biophys. J.* **1996**, *70*, 473–481.
- (17) Becher, B.; Tokunaga, F.; Ebrey, T. G. *Biochemistry* **1978**, *17*, 2293–2300.
- (18) Kriebel, A. N.; Gillbro, T.; Wild, U. P. *Biochim. Biophys. Acta* **1979**, *546*, 106–120.
- (19) Shichida, Y.; Matuoka, S.; Hidaka, Y.; Yoshizawa, T. *Biochim. Biophys. Acta* **1983**, *723*, 240–246.
- (20) Zimányi, L.; Keszthelyi, L.; Lanyi, J. K. *Biochemistry* **1989**, *28*, 5165–5172.
- (21) Váró, G.; Duschl, A.; Lanyi, J. K. *Biochemistry* **1990**, *29*, 3798–3804.
- (22) Zimányi, L.; Cao, Y.; Needleman, R.; Ottolenghi, M.; Lanyi, J. K. *Biochemistry* **1993**, *32*, 7669–7678.
- (23) Lozier, R. H. *Methods Enzymol.* **1982**, *88*, 133–162.
- (24) Váró, G.; Lanyi, J. K. *Biochemistry* **1991**, *30*, 5008–5015.
- (25) Zimányi, L.; Lanyi, J. K. *Biophys. J.* **1993**, *64*, 240–251.
- (26) Oesterhelt, D.; Stoekenius, W. *Methods Enzymol.* **1974**, *31*, 667–678.
- (27) Henry, E. R.; Hofrichter, J. *Methods Enzymol.* **1992**, *210*, 129–192.
- (28) Cao, Y.; Váró, G.; Klinger, A. L.; Czajkowsky, D. M.; Braiman, M. S.; Needleman, R.; Lanyi, J. K. *Biochemistry* **1993**, *32*, 1981–1990.
- (29) Birge, R. R.; Cooper, T. M.; Lawrence, A. F.; Masthay, M. B.; Vasilakis, C.; Zhang, C.-F.; Zidovetzki, R. *J. Am. Chem. Soc.* **1989**, *111*, 4063–4074.
- (30) Li, Q.; Govindjee, R.; Ebrey, T. G. *Proc. Natl. Acad. Sci. U.S.A.* **1984**, *81*, 7079–7082.
- (31) Balashov, S. P.; Govindjee, R.; Ebrey, T. G. *Biophys. J.* **1991**, *60*, 475–490.
- (32) Nagle, J. F.; Zimányi, L.; Lanyi, J. K. *Biophys. J.* **1995**, *68*, 1490–1499.
- (33) Váró, G.; Lanyi, J. K. *Biochemistry* **1990**, *29*, 2241–2250.
- (34) Dancsházy, Z.; Govindjee, R.; Ebrey, T. G. *Proc. Natl. Acad. Sci. U.S.A.* **1988**, *85*, 6358–6361.
- (35) Tokaji, Z.; Dancsházy, Z. *FEBS Lett.* **1992**, *311*, 267–270.
- (36) Einfeld, W.; Pusch, C.; Diller, R.; Lohrmann, R.; Stockburger, M. *Biochemistry* **1993**, *32*, 7196–7215.
- (37) Honig, B.; Greenberg, A. D.; Dinur, U.; Ebrey, T. G. *Biochemistry* **1976**, *15*, 4593–4599.
- (38) Tavan, P.; Schulten, K.; Oesterhelt, D. *Biophys. J.* **1985**, *47*, 415–430.